Structural and magnetic properties of $R(Fe_xMn_{1-x})_{12}$ $(R=Ho,Y)$

J. B. Yang,[1,2] W. B. Yelon,[1] W. J. James,[1] S. Cai,[3] D. Eckert,[2] A. Handstein,[2] K. H. Müller,[2] and Y. C. Yang[4]
[1]*Graduate Center for Materials Research and Department of Chemistry, University of Missouri-Rolla, Rolla, Missouri 65409*
[2]*IFW-Dresden, P. O. Box 270016, D-01171 Dresden, Germany*
[3] *Department of Physics, University of Missouri-Columbia, Columbia, Missouri 65211*
[4]*Department of Physics, Peking University, Beijing 100871, P. R. China*
(Received 29 April 2001; revised manuscript received 10 September 2001; published 24 January 2002)

The crystallographic structures and magnetic properties of $R(Fe_xMn_{1-x})_{12}$ (R=Ho,Y; x=0, 0.2, 0.5, 0.6, 0.7) have been studied using powder neutron diffraction and magnetic measurements. These compounds crystallize in a $ThMn_{12}$-type structure. The rare earths occupy the $2a$ sites, and Fe and Mn atoms are distributed on three nonequivalent sites: $8i$, $8j$, and $8f$. The Mn and Fe atoms are found to exhibit strong site preferences, with the $8i$ sites favoring Mn atoms and the $8f$ sites favoring Fe atoms. $Ho(Fe,Mn)_{12}$ compounds show a noncollinear magnetic structure within the Mn(Fe) sublattice. Spin-glass-like behavior has been observed in these two series. There are two characteristic temperatures for the $Ho(Mn_{1-x}Fe_x)_{12}$; one corresponding to the compensation of the ordered Ho and (Mn,Fe) magnetic moments, and the other to the ordering of the (Mn,Fe) lattice. The uncommon feature of two ordering temperatures in this compound is due to the weak rare-earth (R) transition-metal (T) interaction. The addition of Fe substantially modifies the magnetic interactions, thus increasing the ordering temperature and changing the type of magnetic order of the (Mn,Fe) sublattice.

DOI: 10.1103/PhysRevB.65.064444 PACS number(s): 75.50.−y, 61.12.−q, 75.30.−m, 75.25.+z

I. INTRODUCTION

Ternary $RFe_{12-x}M_x$ (R=rare earth) intermetallic compounds crystallizing in the tetragonal $ThMn_{12}$-type structure can be stabilized when M=Ti, V, Cr, Mo, W, Al, or Si, and x is in the range $1.0 \leqslant x \leqslant 4.0$.[1–6] Contrary to the Fe-rich compounds, YMn_{12} exhibits antiferromagnetic ordering at low temperature.[7] In compounds with magnetic R ions, the R moments couple ferromagnetically below $T_c \approx 5$ K and the Mn moments couple antiferromagnetically below $T_N \approx 100$ K.[7,8] Interesting and peculiar characteristics concerning the magnetic structure, such as antiferromagnetic to ferromagnetic phase transitions, when observed in $Y(Fe_xAl_{1-x})_{12}$ and $R(Fe_xMn_{1-x})_{12}$ (R=Er, Tb).[9,10] Mao *et al.* have observed unusual negative magnetization at low temperatures under field cooling (FC) in $Ho(Fe_{0.6}Mn_{0.4})_{12}$ compounds.[11] Spin-glass-like behavior was observed in $RFe_{12-x}Mo_x$ and $RFe_{12-x}Al_x$ compounds,[12–16] and band calculations were used to explain this phenomenon.[17] In the meantime, many efforts were made to study the intersublattice exchange interactions in rare-earth (R) transition-metal (T) intermetallics.[18,19] However, no results regarding the exchange interaction in $R(Fe,Mn)_{12}$ were reported where an antiferromagnetic T sublattice exists. We thought it would be most interesting to study the magnetic structure and exchange interactions in this kind of material, in the hope that the study would lead to some understanding of the nature of the $3d$-$4f$ interactions in these intermetallic compounds.

In this study, we report on the structural and magnetic properties of $R(Fe_xMn_{1-x})_{12}$ (R=Y, Ho) compounds. The dependence of the magnetic structure on the temperature and Fe content is studied in detail. A spin-glass-like behavior is observed and explained for these compounds. The negative magnetization observed under FC in $Ho(Fe_{0.6}Mn_{0.4})_{12}$ is explained on the basis of neutron diffraction and magnetic measurements. Finally, the mean-field theory is applied to explain the exchange interactions in these compounds.

II. EXPERIMENTAL METHODS

$R(Fe_xMn_{1-x})_{12}$ ingots, with R=Y, Ho and x=0, 0.2, 0.5, 0.6, and 0.7, were prepared by arc melting of 99.9% pure materials in an argon atmosphere, followed by a heat treatment at 1000 °C for one week. The magnetization curves of the bulk samples were measured using a superconducting quantum interference device magnetometer with a field of up to 5 T from 1.8 K to room temperature. A magnetic filed of 0.1 T was used for the FC process. The crystal phase was identified by x-ray diffraction analysis using Co-$K\alpha$ radiation. The magnetic structure was determined using powder neutron diffraction. The neutron diffraction experiments were performed at the University of Missouri-Columbia research reactor using neutrons of wavelength $\lambda = 1.4875$ Å. First, the diffraction patterns were recorded at room temperature where only nuclear scattering was observed. Then the magnetic contributions to diffraction were analyzed from 10 to 300 K. The diffraction data were refined using the program FULLPROF, a program for Rietveld analysis.[20]

III. RESULTS AND DISCUSSIONS

A. Crystallographic structure

Typical neutron diffraction patterns of $Ho(Fe_{0.6}Mn_{0.4})_{12}$ at different temperatures are presented in Fig. 1. The refined data of the structures and magnetic moments are listed in Tables I and II, respectively. All compounds are found to crystallize in a $ThMn_{12}$-type tetragonal structure (the so-called 1:12 phase) space group $I4/mmm$, with the rare earth occupying the $2a$ sites, and Mn(Fe) occupy $8i$, $8j$, and $8f$

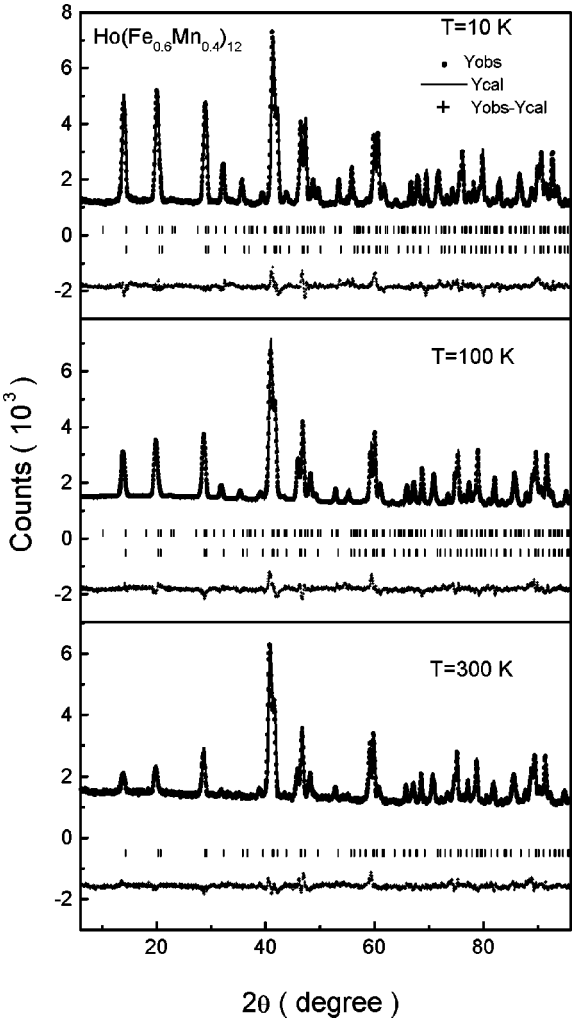

FIG. 1. Observed (Yobs), and calculated (Ycal) neutron diffraction patterns of $Ho(Fe_{0.6}Mn_{0.4})_{12}$ at 10, 100, and 300 K. [The bottom curves (Yobs-Ycal) are the difference between experimental data and refinement data. The vertical bars indicate the magnetic (top) and Bragg (bottom) peak positions. At 300 K, only the Bragg peak positions are shown.]

sites. In some instances, a small amount of β-Mn appears in the compound. The thermal variation of the magnetic reflections can be easily observed as the intensities of the magnetic reflection peaks (at low angle part) decrease drastically with increasing temperature. At 300 K, the magnetic reflection peaks disappear, and only nuclear scattering is observed.

Figure 2 plots the lattice parameters of $R(Fe_xMn_{1-x})_{12}$ (R=Y, Ho) at room temperature. The lattice parameter a decreases with increasing Fe content due to the fact that the Fe atomic radius (1.24 Å) is smaller than of Mn (1.36 Å). The lattice parameter c remains almost constant.

Figure 3 shows the Fe occupation factor dependence on the Fe content. Fe prefers to occupy $8f$ sites, but not to occupy $8i$ sites. This agrees with what is found for $Y(Fe_xMn_{1-x})_{12}$ (Ref. 9) and $Er(Fe,Mn)_{12}$.[10] The reluctance of the Fe atoms to occupy $8i$ sites is consistent with the fact that the RFe_{12} structure does not exist.

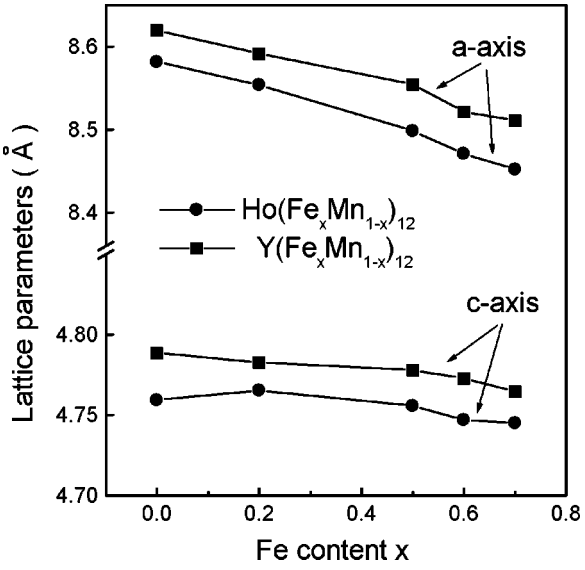

FIG. 2. The lattice parameters a and c of $R(Fe_xMn_{1-x})_{12}$ (R=Y and Ho) as functions of x at room temperature.

B. Magnetic properties

A model similar to the one reported by Morales *et al.*[10] was used to analyze the magnetic structure from the neutron diffraction data of the $Ho(Fe_xMn_{1-x})_{12}$ (x=0.0, 0.2, 0.5, and 0.6). The model leads to a complex noncollinear antiferromagnetic structure on the $3d$ metal sites in the (a,b) plane ($x \leqslant 0.6$), but no moments are observed in the (a,b) plane for the Ho atoms; see Fig. 4. At room temperature, only nuclear scattering is detected for all compositions. However, the diffraction lines with the condition $h+k+l=2n+1$ were observed at low temperature for $x \leqslant 0.6$. In Fig. 5, we display the neutron diffraction patterns of $Ho(Fe_xMn_{1-x})_{12}$ (x=0.0, 0.2, 0.5, 0.6, and 0.7) at 10 K, where some magnetic diffraction lines with $h+k+l=2n+1$ are marked by arrows. The intensities of the marked

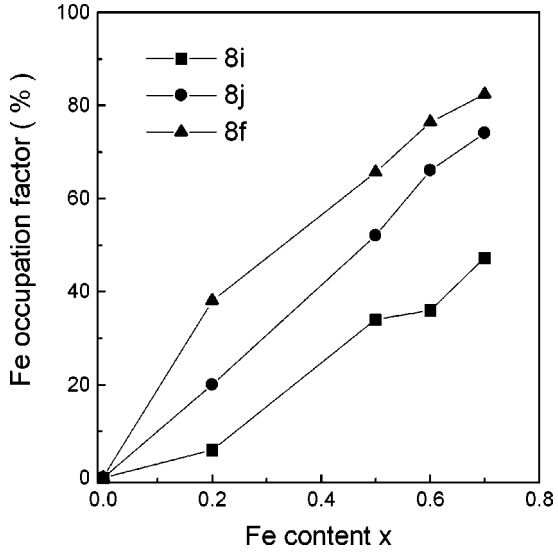

FIG. 3. The Fe occupation factor dependence on the Fe content for $Ho(Fe_xMn_{1-x})_{12}$ at room temperature.

TABLE I. Refinement parameters of $Ho(Fe_xMn_{1-x})_{12}$ at room temperature. a and c are the lattice parameters; V is the unit cell volume; n is the occupation factor; x, y, and z are the fractional position coordinates; R_{wp} is the residual error of the weighted profile; R_{expt} is statistically expected residual error of the entire measured scattering patterns. χ^2 is $[R_{wp}/R_{expt}]^2$.

x	0	0.2	0.5	0.6	0.7
a (Å)	8.5817(2)	8.5543(4)	8.4984(7)	8.4715(1)	8.4528(8)
c (Å)	4.7592(1)	4.7654(7)	4.7557(9)	4.7470(4)	4.7453(0)
V (Å^3)	350.49(7)	348.72(2)	343.48(3)	340.67(6)	339.05(7)
n, Fe,8i(%)	0	6.0(1)	34.0(2)	36.0(1)	47.2(0)
n, Fe,8j(%)	0	20.0(1)	52.0(1)	66.0(1)	74.0(1)
n, Fe,8f(%)	0	38.0(2)	65.6(3)	76.4(1)	82.4(1)
Ho, 2a,x	0	0	0	0	0
Fe/Mn, 8i,x	0.3603(3)	0.3598(3)	0.3569(2)	0.3594(8)	0.3553(3)
Fe/Mn, 8j,x	0.2765(3)	0.2795(5)	0.2759(4)	0.2748(8)	0.2749(4)
Fe/Mn, 8f,x	0.25	0.25	0.25	0.25	0.25
R_{wp}(%)	3.25	2.37	3.64	3.95	5.19
R_{expt}(%)	2.49	2.20	2.59	2.30	2.48
χ^2(%)	1.71	1.16	1.98	2.94	4.38

lines first increase from $x=0.0$ to 0.2, then decrease with increasing x, and finally disappear when $x=0.7$. This indicates that the antiferromagnetic structure of Mn(Fe) sublattice changes to a ferrimagnetic structure as the Fe content x increases. As can be seen from the summarized results in Table II, a ferromagnetic component, attributed to the 3d atoms lying along the c axis, is evidenced for the $0.2 \leqslant x \leqslant 0.6$ samples. However, the Ho atoms always exhibit a magnetic moment along the c axis below the ordering temperature, antiparallel to the ferromagnetic components of Mn(Fe) sublattice, indicating an antiferromagnetic exchange coupling between the 3d and Ho sublattices. The magnetic interaction is different from that of the $ErFe_yMn_{12-y}$ compounds, where no ferromagnetic component along the c axis is found in the 3d sublattice when $y \leqslant 5$.[10] The substitution of the Mn by Fe changes the magnetic structure of the 3d sublattice from antiferromagnetic ($x=0.0$ and 0.2) to ferrimagnetic ($x=0.2$–0.6) or even ferromagnetic when the Fe content is higher than $x=0.7$.

As indicated in Table II, in $HoMn_{12}$, the Mn magnetic moments lie in the (a,b) plane below 77 K, and substitution of Mn by Fe leads to the fact that the magnetization of the

TABLE II. The refined magnetic moments (μ_B) of atoms in $Ho(Fe_xMn_{1-x})_{12}$ ($x=0$, 0.2, 0.5, 0.6, and 0.7) at different temperatures. (z is the component of magnetic moments along the z axis. x,y is the component of magnetic moments in the a,b plane. The total is the sum of the magnetic moment per atom. For all refinements, the magnetic R factor is less than 10% and χ^2 is less than 5%.)

x	T	Ho (2a)	(Mn,Fe) (8j)			(Mn,Fe) (8i)			(Mn,Fe) (8f)		
	(K)	z	x,y	z	total	x,y	z	total	x,y	z	total
0.0	77	0	0.36(7)	0	0.36(7)	0.56(7)	0	0.56(7)	0.23(9)	0	0.23(9)
	10	0	0.54(8)	0	0.54(8)	0.88(8)	0	0.88(8)	0.38(9)	0	0.38(9)
0.2	77	0.64(7)	0.83(5)	−0.46(8)	0.94(7)	1.14(5)	−0.54(5)	1.26(5)	0.10(5)	−0.37(9)	0.40(7)
	10	0.71(5)	0.93(1)	−0.44(5)	1.02(4)	1.43(5)	−0.68(7)	1.58(6)	0.14(4)	−0.48(3)	0.50(4)
0.5	77	2.21(9)	0.02(6)	0.04(6)	0.04(6)	0.39(9)	0.57(9)	0.69(9)	0.03(10)	−0.35(3)	0.35(7)
	10	6.80(7)	0.51(9)	−0.40(2)	0.65(9)	0.35(9)	0.58(8)	0.67(9)	0.04(13)	−0.39(2)	0.39(7)
	150	0.75(5)	0.18(5)	−1.32(10)	1.34(8)	0.45(9)	−0.93(6)	1.03(9)	0.36(8)	−1.01(7)	1.13(5)
0.6	100	4.38(9)	0.25(9)	−0.76(7)	0.81(8)	0.34(3)	−0.18(4)	0.38(6)	0.24(9)	−0.64(4)	0.72(8)
	40	7.46(9)	0.27(5)	−0.70(5)	0.75(4)	0.32(8)	−0.09(3)	0.33(9)	0.12(5)	−0.66(5)	0.68(3)
	10	8.21(5)	0.28(5)	−0.73(3)	0.78(6)	0.38(6)	−0.08(2)	0.39(5)	0.14(4)	−0.72(5)	0.73(9)
	170	2.49(9)	-	−1.59(12)	1.59(12)	-	−0.96(7)	0.96(7)	-	−1.34(7)	1.34(7)
0.7	77	6.19(9)	-	−1.11(7)	1.11(7)	-	−0.45(4)	0.45(4)	-	−1.08(4)	1.08(4)
	10	8.34(10)	-	−1.05(6)	1.05(6)	-	−0.35(3)	0.35(3)	-	−1.03(7)	1.03(7)

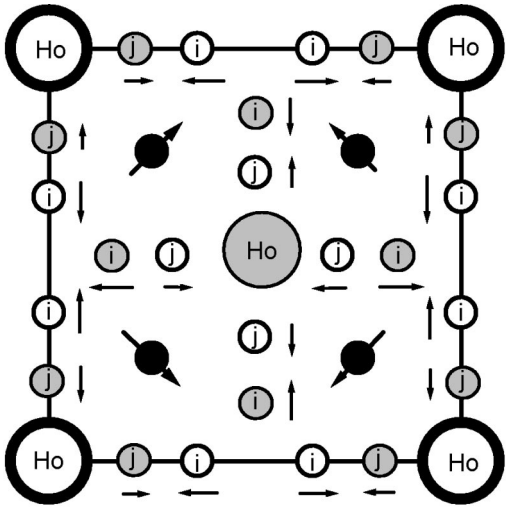

FIG. 4. The magnetic structure of the $Ho(Fe_xMn_{1-x})_{12}$ in the (a,b) plane for $x=0$, 0.2, 0.5, and 0.6. The large circle is the Ho atom, and the small circle is a Mn or Fe atom. The Mn and Fe atoms on the $8i$ and $8j$ sites lie in the planes $z=0$ (open circles) or $z=0.5$ (gray circles). Mn(Fe) atoms on the $8f$ sites lie at $z=0.25$ and 0.75 with black circles.

$3d$ sublattice presents a c-axis component when $x \geqslant 0.2$, but totally flips into the c direction when $x=0.7$. This indicates that the Fe sublattice favors a c-axis anisotropy in the 1:12 compounds, in agreement with the magnetic behavior of $Y(Fe_xM_{1-x})_{12}$ (M=Ti,V,Mo,Si . . .) compounds. At all compositions, the Ho atoms retain a c-axis anisotropy below the Curie temperature T_c. This can only be explained by introducing higher-order terms of the crystal-field coefficients.[7] It can be seen in Table II that the substitution of Mn atoms by Fe atoms leads to a staggered increase in the magnetic moments of the Ho sites due to the increased exchange interaction between Ho and Fe. The change of the magnetic structure of the Mn(Fe) sublattice from antiferromagnetic to ferrimagnetic (ferromagnetic) indicates the substantial change of the exchange interaction in that sublattice.

Figure 6 shows the temperature dependence of the magnetization curves after zero-field cooling (ZFC) and FC for $R(Fe_xMn_{1-x})_{12}$ (R=Y, Ho). The difference between the FC and ZFC curves indicates the appearance of irreversibility at temperatures below 100 K for the Ho-containing compounds and 50 K for the Y-containing compounds. Especially for $Ho(Fe_xMn_{1-x})_{12}$, the FC and ZFC curves exhibit totally different features at low temperature, suggesting a spin-glass-like behavior. A spin-glass-like behavior was observed in the 1:12 compounds $RFe_{10}Mo_2$ and YFe_xAl_{12-x}.[14,15] The experimental results suggest that the ordering in $R(Fe,Mo)_{12}$ is established by spin freezing in a noncollinear magnetic configuration. According to the neutron diffraction data, there is a negative magnetic interaction in the (a,b) plane of the Mn (Fe) sublattices, a positive interaction along the c axis between the Mn(Fe) sublattices, and a negative interaction between the Mn(Fe) and Ho sublattices along the c-axis. The large difference between the ZFC and FC curves of $Ho(Fe_xMn_{1-x})_{12}$ and $Y(Fe_xMn_{1-x})_{12}$ compounds at low temperatures is attributed to the magnetic ordering of Ho atoms which possess a very large moment and anisotropy at low temperatures. Therefore, the Ho-(Mn)Fe interactions should play a key role in the spin-glass-like behavior.

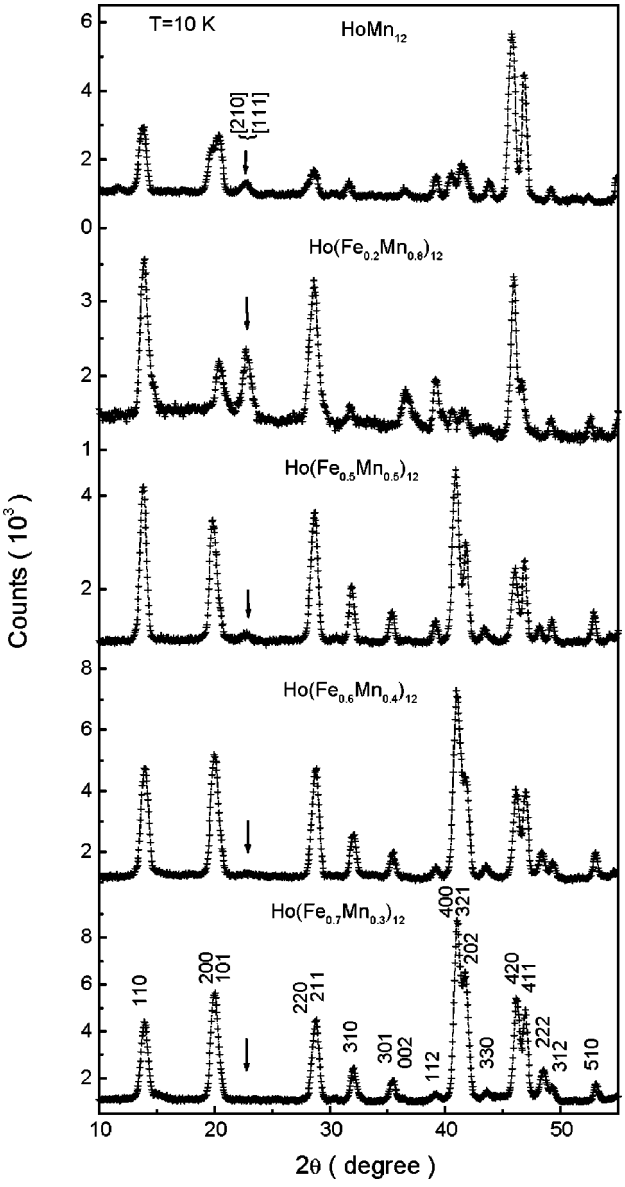

FIG. 5. The neutron diffraction patterns of $Ho(Fe_xMn_{1-x})_{12}$ ($x=0.0$, 0.2, 0.5, 0.6, and 0.7) measured at 10 K. (The reflection lines of $h+k+l=2n+1$ were marked with arrows.)

Table III shows that there are two characteristic temperatures characterizing magnetic ordering in $Ho(Fe_xMn_{1-x})_{12}$ when $x \neq 0.0$. A comparison between the magnetization of $Ho(Fe_xMn_{1-x})_{12}$ and $Y(Fe_xMn_{1-x})_{12}$ suggests that the higher characteristic temperature (T_c or T_N) corresponds to the ordering of the Fe-Mn sublattice, whereas the second characteristic temperature (T_R) is a compensation point resulting from the magnetic ordering of the Ho atoms. The increase of the ordering temperature with increasing Fe content, is attributed to the enhanced R-Fe(Mn) interactions. A further interesting feature can be seen in Fig. 6 for the field-cooling $Ho(Fe_{0.6}Mn_{0.4})_{12}$ sample, where a negative magneti-

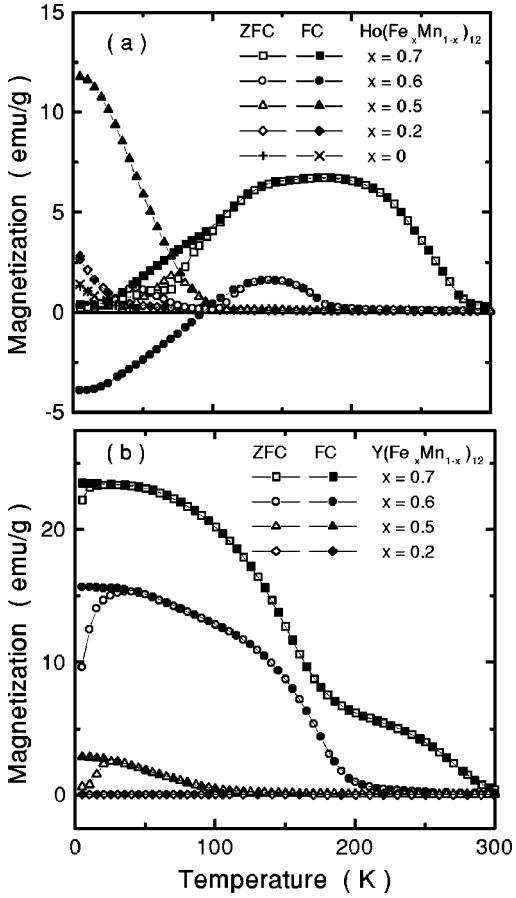

FIG. 6. The temperature dependence of the magnetization curves under zero-field cooling (ZFC) and field cooling (FC) for $R(\mathrm{Fe}_x\mathrm{Mn}_{1-x})_{12}$ (R=Y and Ho). The measured field is 0.1 T.

zation value is observed below 100 K. This phenomenon is also field dependent,[11] where a larger measured field leads to non-negative values. According to the neutron diffraction data at low temperatures, the magnetization of the Ho atom is along the *c* axis below the Curie temperature, while the magnetization of the Mn(Fe) sublattice also has a *c*-axis component. The Ho and Mn (Fe) atoms have negatively exchange couplings, and the Ho atoms possess a magnetic moment as large as $4.4\mu_B$/atom at 100 K. However, Mn(Fe) has a magnetic moment in the range $0.4\mu_B$ to $0.8\mu_B$/atom, and a ferrimagnetic coupling exists within the Mn(Fe) sublattice due to the substitution of Mn by Fe. The ZFC curve of $\mathrm{Y}(\mathrm{Fe}_{0.6}\mathrm{Mn}_{0.4})_{12}$ indicates the ferrimagnetic character. Upon field cooling from room temperature, the magnetic moments are aligned with the external field direction below the Curie temperature. The Fe(Mn) sublattice orders first at higher temperature with magnetic moments in the same direction as the external field, and larger than the magnetic moments of the Ho sublattice. From measurements at low temperature (1.8 K), the Ho sublattice is found to possess a larger magnetic moment in the opposite direction to that of the Mn(Fe) sublattice due to the negative exchange coupling between Ho and Fe(Mn) sublattices. Accordingly, a negative value of the total magnetization will be induced if the external field is lower than the anisotropy field of the Ho sublattice. The Ho

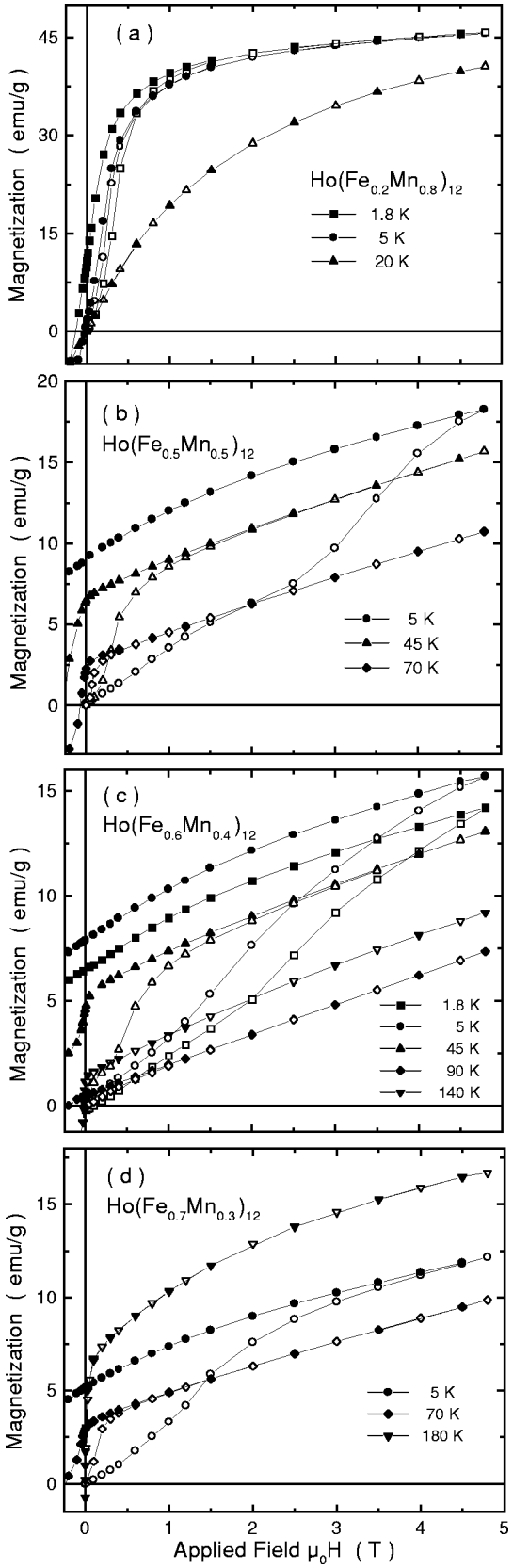

FIG. 7. The field dependence of the magnetization of $\mathrm{Ho}(\mathrm{Fe}_x\mathrm{Mn}_{1-x})_{12}$ (x=0.2, 0.5, 0.6, and 0.7) at different temperatures under ZFC (solid symbols) and FC (open symbols).

TABLE III. The characteristic temperatures of $Ho(Fe_xMn_{1-x})_{12}$ and $Y(Fe_xMn_{1-x})_{12}$. (T_N is the Néel temperature, T_c is the Curie temperature, and T_R is the compensation temperature.)

		$x=0.0$	$x=0.2$	$x=0.5$	$x=0.6$	$x=0.7$
Y	$T_c(T_N)$ (K)	120(T_N)	125(T_N)	115	210	300
Ho	T_R (K)	1.6	3.1	50	100	140
	T_c (K)	5	27	102	195	300

magnetic moment decreases with increasing temperature, so the absolute value of the total magnetization decreases, and reaches zero when the contribution from the Ho sublattice is equal to that of the Mn(Fe) sublattice. A further increase in temperature leads to a rapid decrease in the Ho magnetic moment, and the magnetic moment of the Mn(Fe) sublattice reaches a maximum at 150 K due to the ferrimagnetic coupling. At higher temperatures, only the Mn(Fe) sublattice contributes to the total magnetization, and the magnetization decreases to zero at the Curie temperature.

In the case of ZFC measurements, the negative exchange coupling between the Ho and Mn(Fe) sublattices, connected with the large magnetic anisotropy of the Ho sublattice, leads to a very small induced magnetization under a small measured field. As the temperature increases, the magnetization of the Ho sublattice decreases, and the total magnetization reaches its maximum at a point where the Ho and Fe(Mn) sublattices produce a large component along the external field direction. The total magnetization then decreases due to the rapid decrease in the Ho magnetic moments and the magnetization versus temperature M-T curves measured after ZFC and FC in Fig. 6 coincide because spin freezing is overcome. At higher temperatures, the Fe(Mn) sublattice becomes dominant in the total magnetization. The total magnetization reaches another maximum when the ferrimagnetic (Fe-Mn) sublattice has its highest values of the magnetization and the Ho magnetization is small. Then all moments decrease to zero at the Curie temperature.

As shown in Fig. 6, when $x<0.5$, the Ho sublattice dominates the total magnetization of the compounds in the low temperature range, such that when the M-T curves change from $x=0.0$ to 0.5, an increase of ordering temperature in the Ho sublattice arises caused by an increase of the R-Fe interaction. For $x=0.7$ where the Fe(Mn) sublattice dominates the total magnetization of the compound in the high-temperature range, the total magnetization becomes small at low temperatures due to the ordering of the Ho magnetic moments, whereby a ferrimagnetic structure is formed between the Ho and (Fe,Mn) sublattices. However, in that case, in the FC experiment the net magnetization of the Ho sublattice is not large enough to overcompensate for the positive (Fe,Mn) magnetization, i.e., the total magnetization does not become negative.

Figure 7 shows the field dependence of the magnetization after ZFC and FC at different temperatures for the $Ho(Fe_xMn_{1-x})_{12}$ compounds. The magnetization curves of the $x=0.5$, 0.6, and 0.7 samples show special features. For example, the low-temperature magnetization increases slowly in the low-field region, and a sharp increase results when the external field is larger than some critical value. This is attributed to an increase of the anisotropy field and coercivity at low temperatures. At 45 K a relatively soft magnetic behavior at small fields can be seen, which corresponds to the peak between 30 and 70 K in the ZFC cures of Fig. 6.

The magnetization curves measured after FC and ZFC for $x=0.6$ samples show different features, again, as shown in Fig. 7(c). The difference between the FC and ZFC magnetization values remains almost constant with an applied field up to 5 T at 1.8 and 5 K. In Fig. 8 typical hysteresis loops of $Ho(Fe_{0.6}Mn_{0.4})_{12}$ measured at 1.8 K after FC and ZFC are presented. For the FC sample, a shift of the hysteresis loop is observed which is related to the negative branch to the FC curve in Fig. 6. Obviously a uniaxial magnetic anisotropy has been induced during FC which, at a temperature 1.8 K, cannot be removed by an external field as large as 5 T.

C. Exchange interactions

In the rare-earth (R)–transition-metal (T) intermetallics, there are normally three types of interaction, R-R interaction

TABLE IV. The molecular field (B^R_{exch}) and molecular field coefficients (n_{RT}, n_{RR}) of RMn_{12} and $Ho(Fe_xMn_{1-x})_{12}$ derived from analysis of the ordering temperatures.

	Gd	Tb	Dy	Ho	Er
B^R_{exch} (T)	2.5	2.0	0.9	0.6	0.6
n_{RR}(T f.u./μ_B)	0.31	0.20	0.09	0.06	0.05
	$Ho(Fe_xMn_{1-x})_{12}$				
x	0.0	0.2	0.5	0.6	0.7
B^R_{exch} (T)	0.6	1.3	19.8	39.7	55.6
n_{RT} (T f.u./μ_B)	–	0.05	3.75	5.01	5.71

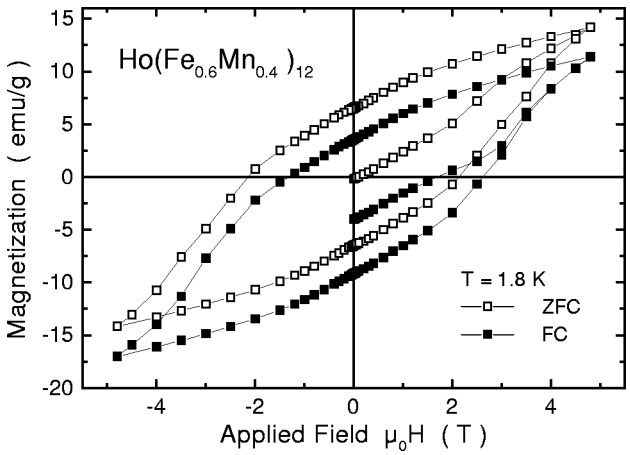

FIG. 8. Hysteresis loops of $Ho(Fe_{0.6}Mn_{0.4})_{12}$ measured at 1.8 K after field cooling (FC) and zero field cooling (ZFC).

between the R magnetic moments, R-T interaction between the magnetic moments of R and T atoms, and T-T interaction between the magnetic moments of T atoms. From a knowledge of the ordering temperatures, we are able to study these exchange interactions. For RMn_{12} compounds, the Mn sublattice is antiferromagnetic, and , for symmetry reasons, the Mn-Mn interaction cancels on the Ho sites; consequently R-Mn interaction can be ignored.[7] The exchange field experienced by the Ho moments due to the Ho sublattice can be obtained by means of the mean-field expression[19,21]

$$B_{exch}^{R}=\frac{3k_BT_R}{g_R(J+1)\mu_B}=n_{RR}M_R, \tag{1}$$

where B_{exch}^{R} is the molecular field experienced by the rare-earth atoms, g_R is the Landé factor of the R^{3+} ion, T_R is the ordering temperature of RMn_{12}, n_{RR} is the intrasublattice molecular field coefficient, and M_R is the magnetic moment of the R sublattice. Using the experimental values of $T_R=1.6$ K and $M_R=10.5\mu_B$/f.u. for $HoMn_{12}$, we find that the $B_{exch}^{R}=0.6$ T and $n_{RR}=0.06$ T f.u./μ_B, which is of the same order as obtained in the heavy rare-earth RNi_5 compounds.[22] In Table IV, for comparison, the B_{exch}^{R} and n_{RR} values are given for RMn_{12} with $R=$ Gd, Tb, Dy, and Er, using data from Ref. 7. As can be seen from the table, $GdMn_{12}$ shows the largest R-R interaction which is consistent with other R-T compounds.

When Fe is substituted for Mn, the T sublattice shows a net magnetization due to the ferrimagnetic structure, so the rare earth experiences an additional molecular field due to the T-R interactions, and Eq. (1) can be written as

$$B_{exch}^{R}=\frac{3k_BT_R}{g_R(J+1)\mu_B}=n_{RR}M_R+n_{RT}M_T, \tag{2}$$

where T_R is the compensation temperature, n_{RT} is the intrasublattice molecular-field coefficient, and M_T is the magnetic moment of the T sublattice. If the value of n_{RR} is assumed to be the same as for $HoMn_{12}$, the estimated values of n_{RT} can be obtained using Eq. (2), and these values are listed in Table IV. From the table, one can see that the addition of Fe increases the exchange interaction between the Ho and Mn(Fe) sublattices. The Fe atoms also change the interaction between the Mn atoms, namely, from antiferromagnetic to ferrimagnetic.

The Curie temperature of $HoMn_{12}$ is the ordering temperature of Ho due to the Ho-Ho interaction, and can be written as[21]

$$T_R=2Z_{RR}A_{RR}G_R/3k_B. \tag{3}$$

Similarly, T_T represents the contribution of the ordering temperature due to the T-T interaction:

$$T_T=2Z_{TT}A_{TT}G_T/3k_B, \tag{4}$$

where G_R is the de Gennes factor $(g_R-1)^2\mathbf{J}(\mathbf{J}+1)$ for the rare earth. $A_{ij}(i,j=R,T)$ is the microscopic exchange-coupling parameter. $Z_{RR}=8$ and $Z_{TT}=10$ are the number of R nearest neighbors of the R ions, and the number of T nearest neighbors of the T ions, respectively. G_T is the corresponding de Gennes factor for the transition metal. $[G_T=S_T(S_T+1)]$. Using Eqs. (3) and (4), A_{RR} is found to be 2.5×10^{-24} J for $HoMn_{12}$, and A_{TT} is found to be 1.1×10^{-21} J for $Ho(Fe_{0.7}Mn_{0.3})_{12}$. It is evident that the T-T interactions are much stronger than the R-R interactions.

In summary, the R-R and R-T interactions in these compounds are very weak as compared with the R-Fe and R-Co compounds. The weak R-T interactions do not allow rare-earth magnetism to persist up to high temperatures. Especially in RMn_{12} compounds, the effects of the crystal field on the rare-earth atoms are much stronger than the exchange interactions of R-R interaction. The Ho atoms exhibit a c-axis anisotropy which is attributed to the higher order crystal-field terms. The weak R-T interactions also are relative to the complex magnetic structure which leads to a spin-glass-like behavior in $Ho(Fe_xMn_{1-x})_{12}$ compounds.

IV. CONCLUSIONS

Upon the substitution of Mn by Fe, the Curie temperature (T_c), saturation magnetization (M_s) and anisotropy of the $R(Fe_xMn_{1-x})_{12}$ ($R=$ Y, Ho) compounds increase markedly. Two characteristic temperatures have been observed in the $Ho(Fe_xMn_{1-x})_{12}$ when x is larger than 0.2, one corresponding to compensation connected with the magnetic ordering of rare-earth Ho atoms, and the other corresponding to the Fe(Mn) sublattice ordering. The R-T interaction are weak in these compounds due to antiferromagnetic or ferrimagnetic interactions in the transition metals sublattice. Both Ho and Y compounds show spin-glass-like behavior due to the weakness of the R-T interactions which lead to a noncollinear magnetic structure. A negative magnetization has been observed on field-cooled samples for $x=0.6$ below 100 K, which is explained by the increase of the Ho magnetic moments with decreasing temperature. The Ho moments are antiferromagnetically coupled to the (Fe,Mn) magnetization. The negative direction of the Ho moments is stabilized by a strong anisotropy field.

ACKNOWLEDGMENTS

One of the authors (J.B.Y.) acknowledges the financial support of the Alexander von Humboldt Foundation. The financial support of the National Science Foundation for Grant No. DMR-9614596 and the Defense Advanced Research Projects Agency for Grant No. DAAG 55-98-1-0267 is acknowledged. This work was partially supported by the State Key Project of Fundamental Research and the National Science Foundation of China.

[1] Y. C. Yang, B. Kebe, W. J. James, J. Deportes, and W. Yelon, J. Appl. Phys. **52**, 2077 (1981).
[2] K. H. J. Buschow, J. Appl. Phys. **63**, 3130 (1988).
[3] K. H. J. Buschow, Rep. Prog. Phys. **54**, 1123 (1991).
[4] K. Ohashi, Y. Tawara, R. Osugi, and M. Shimao, J. Appl. Phys. **64**, 5714 (1988).
[5] H. S. Li and J. M. D. Coey, in *Handbook of Magnetic Materials*, edited by K. H. J. Buschow (Elsevier, Amsterdam, 1991), Vol. 6.
[6] W. Suski, in *Handbook on the Physics and Chemistry of Rare Earth*, edited by K. A. Gscheidner, Jr. and L. Eyring (Elsevier, Amsterdam, 1996), Vol. 22.
[7] J. Deportes, D. Givord, R. Lemaire, and H. Nagai, Physica B & C **86-88**, 69 (1977).
[8] N. Okamoto, H. Nagai, H. Yoshie, A. Tsujimura, and T. Hihara, J. Magn. Magn. Mater. **70**, 299 (1987).
[9] Y. C. Yang, G. L. Long, W. J. James, and R. Yeh, J. Appl. Phys. **53**, 1958 (1982).
[10] M. Morales, M. Artigas, M. Bacmann, D. Fruchart, J. L. Soubeyroux, and P. Wolfers, J. Alloys Compd. **263-267**, 134 (1997).
[11] W. H. Mao, J. B. Yang, B. P. Cheng, and Y. C. Yang, Solid State Commun. **109**, 655 (1999).
[12] I. A. Al-Omari, S. S. Jaswal, A. S. Fernando, D. J. Sellmyer, and H. H. Hamdeh, Phys. Rev. B **50**, 12 665 (1994).
[13] M. Anagnostou, E. Devlin, V. Psyharis, A. Kostikas, and D. Niarchos, J. Magn. Magn. Mater. **131**, 157 (1994).
[14] C. Christides, A. Kostikas, G. Zouganelis, V. Psyharis, X. C. Kou, and R. Grössinger, Phys. Rev. B **47**, 11 220 (1993).
[15] I. Felner and I. Nowik, J. Magn. Magn. Mater. **58**, 169 (1986); **54-57**, 163 (1986).
[16] J. A. Paixão, M. Ramos Silva, S. A. Sørensen, B. Lebech, G. H. Lander, P. J. Brown, S. Langridge, E. Talik, and A. P. Goncalves, Phys. Rev. B **61**, 6176 (2000).
[17] R. Lorenz, J. Hafner, S. S. Jaswal, and D. J. Sellmyer, Phys. Rev. Lett. **74**, 3688 (1995).
[18] N. H. Duc, in *Handbook on the Physics and Chemistry of Rare Earth*, edited by K. A. Gscheidner, Jr. and L. Eyring (Elsevier, Amsterdam, 1997), Vol. 24, Chap. 163, p. 339, and references therein.
[19] J. P. Liu, F. R. de Boer, P. F. de Châtel, R. Coehoorn, and K. H. J. Buschow, J. Magn. Magn. Mater. **132**, 159 (1994).
[20] J. Rodriguez-Carvajal, ''Program: Fullprof,'' Version 3.0.0, 1995.
[21] N. H. Duc, T. D. Hien, D. Givord, J. J. M. Franse, and F. R. de Boer, J. Magn. Magn. Mater. **124**, 305 (1993).
[22] A. Szewczyk, R. J. Radwanski, J. J. M. Franse, and H. Nakotte, J. Magn. Magn. Mater. **104-107**, 1319 (1992).